COLLECTIVE MODES IN NUCLEAR MATTER

A thesis submitted in partial fulfillment of the requirement
for the degree of Bachelor of Science with Honors in
Physics from the College of William and Mary in Virginia,

by

Cihan Akcay

Accepted for _____
(Honors, High Honors or Highest Honors)

_____
Advisor: Dr. Walecka

_____
Dr. Griffioen

_____
Dr. Carone

_____
Dr. Spitkovsky

The College of William and Mary
Williamsburg, Virginia
April 2002

Abstract

We consider uniform nuclear matter (or neutron matter) made of equal number of protons and neutrons (or simply neutrons) and study collective modes in this medium at zero temperature. Collective modes are fluctuations (i.e. sound waves) that propagate through the nuclear medium. We examine the propagation of these elementary excitations through this uniform nuclear medium and neutron matter using linear and the more realistic non-linear models. We first derive a set of non-linear equations, linearize them, and analytically solve these linear equations to study the propagation and velocity of various modes. We then investigate how the zero-sound disturbance travels in nuclear media by numerically solving the non-linear differential equations that depict our system. Again we first linearize these differential equations and consider small oscillations about the equilibrium. Then we solve the full non-linear case. We let the wave amplitude grow, and observe how this growing amplitude transforms to a shock wave due to the non-linearities in the system.

Acknowledgements

I would first like to thank my advisor Professor Walecka for his knowledge of physics, guidance and infinite wisdom. I would also like to thank Professor Griffioen for all the help and constructive criticism that he offered and finally I wish to thank my friend Patrick Meade for helping me with all my computer-related problems.

Contents

1 INTRODUCTION

We study here the propagation of elementary excitations through uniform nuclear matter at zero temperature in the approximation that it can be treated as a semi-classical, relativistic fluid through the use of the "mean-field" theory (MFT)[1]. We define an irrotational velocity field $\mathbf{v} = -\nabla\mathbf{\Psi}$ (here Ψ is the velocity potential) describing our collective modes, then solve the system of non-linear equations, which is described by using a nuclear fluid-dynamical model [2, 3]. Collective modes are elementary excitations about the equilibrium. They are described by allowing the meson fields and nucleon densities to acquire a time-dependence [2, 4]. The nucleon motion modifies the source term in the meson field equations producing corresponding time-dependent changes in the meson fields [2]. The goal is to see how nuclear matter reacts to these collective excitations. This work is quite applicable to describing phenomena such as stellar explosions leading to the formation of neutron stars or high-energy heavy-ion collisions. One can achieve this by applying the "mean-field" theory approach to a chosen system and solve the equation of state at all temperatures rather than simply considering T = 0 [5].

The elementary excitations that are of greatest interest to us are generated by what we call zero sound, which is the fundamental sound wave travelling through nuclear media. It is different from ordinary sound in that it does not require collisions in a gas in thermodynamic equilibrium for propagation, and it is the only sound that occurs at zero temperature. It is a collective mode sustained by the coherent self-consistent interaction arising from neighboring particles; thus it occurs in a collisionless regime and is due to quantum mechanical pressure [6].

We will show that once coupled to the scalar meson field, as described by our models, the zero sound collective mode will no longer exhibit its usual linear behavior defined by the dispersion relation: $w = |\mathbf{k}|v$. Using three different sets of parameters determined experimentally, the linear L2, and the non-linear NLC, and Q1, we will

calculate the group and phase velocities at which these zero sound modes propagate in nuclear and neutron matter. Once we are satisfied with our results, we will numerically attempt to solve the non-linear equations of the propagating modes and get expressions for the velocity potential and Fermi momentum of the nuclear matter, which depict how the wave evolves in time. This we will do by first linearizing these equations. Then we will actually keep the non-linear terms and see if we can observe a shock front forming. Since the linear case is a simplified version of the non-linear problem, it is crucial that we be able to recover the same initial results from both systems.

2 QHD

We know that the only consistent framework for discussing the relativistic many-body system is relativistic quantum field theory based on a local Lagrangian density, which describes the state of our system [7]. Using this approach, we have to specify our generalized coordinates (fields) and hadronic degrees of freedom, baryons and mesons to create a simple model of nuclear matter. In analogy with QED, it is convenient to refer to local relativistic quantum field theories based on hadronic degrees of freedom as quantum hadrodynamics (QHD) [1]. QHD can be regarded as a low energy (long wavelength) effective theory of QCD, since it embodies all the principles and symmetries of QCD.

2.1 QHD-I

We will start by concentrating on a simplified model of QHD, which contains fields for baryons

$$\psi = \begin{pmatrix} p \\ n \end{pmatrix}$$

and neutral fields for mesons, ϕ and V_λ. Here ϕ is a neutral Lorentz scalar field coupled to the scalar density $\bar{\psi}\psi$, and V_λ is a neutral Lorentz vector field coupled to the conserved baryon current $\bar{\psi}\gamma_\mu\psi$ [1]. These choices are motivated by several considerations. First, ϕ and V_λ provide the smoothest average nuclear interactions and should describe the dominant features of the bulk properties of nuclear matter. Second, in the static limit of infinitely heavy baryons sources, these exchanges give rise to an effective NN interaction of the form

$$V_{static} = \frac{g_v^2}{4\pi}\frac{e^{-m_v r}}{r} - \frac{g_s^2}{4\pi}\frac{e^{-m_s r}}{r} \tag{1}$$

With the appropriate choice of coupling constants and masses this potential describes the main features of the NN interaction: a short-range repulsion due to ω-pion exchange, and a long-range attraction due to α-pion exchange, which are responsible for the saturation properties of nuclear matter [8] The Lagrangian density for this system (with $\hbar = c = 1$) then is as given in [1]

$$\begin{aligned}\mathcal{L} = &-\frac{1}{4}F_{\mu\nu}F^{\mu\nu} + \frac{1}{2}m_v^2 V_\mu V^\mu + \frac{1}{2}[\partial_\mu\phi\partial^\mu\phi - m_s^2\phi^2] - \frac{1}{3!}\Omega\phi^3 \\ &-\frac{1}{4!}\lambda\phi^4 + \bar{\psi}[\gamma_\mu(i\partial^\mu - g_v V_\mu) - (M - g_s\phi)]\psi\end{aligned} \tag{2}$$

where [1] $F^{\mu\nu}$ is the vector meson field tensor, which is defined by

$$F^{\mu\nu} \equiv \partial^\mu V^\nu - \partial^\nu V^\mu \tag{3}$$

Note that the higher order terms in ϕ, which represent the scalar self-interaction, make the Lagrangian in Eq. 2 consistent with renormalization [1]. These self-interaction terms are not included in the original version of the model, which uses the L2 (linear) set of parameters. We can now obtain the field equations from the Lagrangian in Eq. 2

$$\partial_\nu F^{\nu\mu} + m_v^2 V^\mu \;\; = \;\; g_v\bar{\psi}\gamma^\mu\psi \tag{4}$$

[1]The metric used in this study is (1,-1,-1,-1) and our gamma matrices satisfy the following anti-commutation relation: $\{\gamma^\mu, \gamma^\nu\} = 2g^{\mu\nu} \times \mathbf{1}_{nxn}$

$$(\partial_\mu \partial^\mu + m_s^2)\phi + \frac{1}{2}\Omega\phi^2 + \frac{1}{6}\lambda\phi^3 = g_s\bar{\psi}\psi \quad (5)$$

$$[\gamma^\mu(i\partial_\mu - g_V V_\mu) - (M - g_s\phi)]\psi = 0 \quad (6)$$

The first of these field equations is just the relativistic form of Maxwell's equations, $\partial_\nu F^{\mu\nu} = J^\mu$, with conserved baryon current $B_\mu \equiv (\rho_B, \mathbf{B}) = \bar{\psi}\gamma^\mu\psi$ as source and a massive V_μ. The second field equation is the Klein-Gordon equation for the scalar field with scalar density $\bar{\psi}\psi$ as source with the non-linear couplings included [1, 9]. The last equation is the Dirac equation for the baryon field with the meson fields entering in a minimal fashion [1, 9].

3 RELATIVISTIC MEAN FIELD THEORY (RMFT)

Since QHD deals with strong baryon sources it cannot be solved perturbatively. RMFT is an approximate nonperturbative solution that can serve as an initial tool for studying the system described by the Lagrangian in Eq. 2. Consider a large box of volume V filled uniformly with B baryons at zero temperature. The baryon number is conserved, as a result so is the baryon density $\rho_B = B/V$, where $B = \int d^3x B^0$. Now if one shrinks the box, one naturally observes an increase in the baryon density, which also causes the source terms on the right-hand side of Eqs. 4 and 5 to get large. As in the case of QED, when there are many quanta (photons in QED) present, we can use classical fields and make classical approximations to solve problems. Similarly, when the source gets strong one can replace the meson fields by classical fields and the sources by their expectation values [1, 9]. In the limit of large ρ_B, the following transformation occurs [1, 9]

$$\phi \rightarrow \langle\phi\rangle = \phi_0 \quad (7)$$

$$V^\mu \rightarrow \langle V^\mu\rangle = (V_0, \mathbf{0}) \quad (8)$$

Once we approximate the meson fields by the constant classical fields, the Lagrangian becomes

$$\mathcal{L}_{MFT} = \frac{1}{2}m_v^2 V_0^2 - \frac{1}{2}m_s^2\phi_0^2 - \frac{1}{3!}\Omega\phi_0^3 - \frac{1}{4!}\lambda\phi_0^4 + \bar{\psi}[i\partial^\mu\gamma_\mu - g_v V_0\gamma_0 - M^*]\psi \quad (9)$$

where the couplings constants g_s and g_v are the parameters in the theory that are adjusted to fit the binding energy and density of nuclear matter, and $M^* \equiv M - g_s\phi_0$ is the effective mass of the nucleon. The MFT field equations then are

$$\begin{aligned} m_s^2\phi_0 + \frac{1}{2}\Omega\phi_0^2 - \frac{1}{6}\lambda\phi_0^3 &= g_s\langle\bar{\psi}\psi\rangle & (10)\\ V_0 = \frac{g_v}{m_v^2}\langle\psi^\dagger\psi\rangle &\equiv \frac{g_v}{m_v^2}\rho_B & (11)\\ [i\gamma_\mu\partial^\mu - \gamma_0 g_v V_0 + M^*]\psi(\mathbf{x},t) &= 0 & (12)\end{aligned}$$

Note that if we let the additional nonlinear terms in ϕ_0 go to zero, Eq. 13 yields an exact expression for the scalar density

$$\phi_0 = \frac{g_s}{m_s^2}\langle\bar{\psi}\psi\rangle \equiv \frac{g_s}{m_s^2}\rho_s \quad (13)$$

Thus, we have solved the two field equations in terms of the scalar and meson fields. The third equation is just the free Dirac equation with the energy now shifted by $g_v V_0$ and the baryon mass by $g_s\phi_0$ due to the presence of the vector and scalar fields, V_0 and ϕ_0. So the new baryon mass is the effective mass $M^* \equiv M - g_s\phi_0$ and the energy is

$$E = g_v V_0 \pm (\mathbf{p}^2 + M^{*2})^{1/2} \quad (14)$$

For uniform nuclear matter, the ground state is obtained by filling the energy levels up to a Fermi momentum k_F with spin-isospin degeneracy of $\gamma = 4$ [9]. The energy density, $\epsilon = E/V$, pressure p, and baryon density ρ_B can be obtained after quantizing the fermion field (meson fields here are classical therefore are not quantized) and taking the expectation value of the Hamiltonian. Hence, one obtains the following results (See appendices A and B)

$$\rho_B = \frac{\gamma}{(2\pi)^3}\int_0^{k_F} d^3k = \frac{\gamma}{6\pi^2}k_F^3 \quad (15)$$

$$\varepsilon = \frac{g_v^2}{2m_v^2}\rho_B^2 + \frac{m_s^2}{2g_s^2}(M-M^*)^2 + \frac{\Omega}{6g_s^3}(M-M^*)^3 + \frac{\lambda}{24g_s^4}(M-M^*)^4 + \frac{\gamma}{(2\pi)^3}\int_0^{k_F} d^3k(\mathbf{k}^2 + M^{*2})^{1/2} \tag{16}$$

$$p = \frac{g_v^2}{2m_v^2}\rho_B^2 - \frac{m_s^2}{2g_s^2}(M-M^*)^2 - \frac{\Omega}{6g_s^3}(M-M^*)^3 - \frac{\lambda}{24g_s^4}(M-M^*)^4 + \frac{1}{3}\frac{\gamma}{(2\pi)^3}\int_0^{k_F} d^3k\frac{\mathbf{k}^2}{(\mathbf{k}^2 + M^{*2})^{1/2}} \tag{17}$$

Here the density, ρ_B is the "normal-ordered" baryon number operator , which counts the number of baryons minus the number of antibaryons relative to the vacuum, and becomes the charge operator when coupled to an electric or baryonic field. There is also a correction term, $\delta\mathcal{H}$ in our Hamiltonian, which is normally called the zero-point energy. It represents the difference of energy of a filled negative-energy Fermi sea of baryons with mass M^* and that of a filled-negative energy Fermi sea of baryons of mass M [1, 9]. It arises from placing the operators in normal order. The possible effects of $\delta\mathcal{H}$ are discussed in [4], here we simply neglect this term.

As Walecka explains in [9] there are only two parameters in this MFT of nuclear medium and we can fit them to the two properties of nuclear matter that can be determined experimentally, the binding energy and density. This result yields the numerical values for the coupling constants g_s and g_v, and we see that the Lorentz (relativistic) structure of the interaction provides an additional saturation mechanism and leads to a new energy scale in the problem. The small nuclear binding energy (15.75 MeV) arises from the cancellation between the large scalar attraction (-400 MeV) and vector repulsion (350 MeV) [1, 9]. Note that the neutron matter ($\gamma = 2$) is unbound. As the nuclear density increases M decreases, the scalar source becomes much smaller than the vector source [1, 9], causing the attractive forces to saturate. We can look at the scalar source more closely with the aid of thermodynamics. At fixed volume and density, the system minimizes its energy, $(\partial\varepsilon/\partial M^*)_{V,B} = 0$. Im-

posing this condition on Eq. 16 yields

$$M^* = M - \frac{g_s^2}{m_s^2}\rho_s + \frac{\Omega}{2g_s m_s^2}(M - M^*)^2 + \frac{\lambda}{6g_s^2 m_s^2}(M - M^*)^3 \tag{18}$$

This is the self-consistency equation for the effective mass, M* that can be solved at each value of k_F. Here ρ_s represents the scalar density and is defined by

$$\rho_s = \frac{\gamma}{(2\pi)^3}\int_0^{k_F} d^3k \frac{M^*}{(\mathbf{k}^2 + M^{*2})^{1/2}} \tag{19}$$

The solution of the self-consistency equation yields an effective mass that decreases as a function of density [1, 9]. The reader must note that even at ordinary densities where the nuclear matter saturates (roughly 1.4 fm^{-1}), M* is significantly smaller than M due to the large scalar field $g_s\phi_0$, which is approximately 400 MeV at that density.

4 COLLECTIVE MODES

4.1 NUCLEAR MATTER

We wish to study the behavior of collective modes in nuclear matter. Since the baryon density is large, the energy, pressure densities and fluid velocity field $\mathbf{v}$ are all macroscopic quantities [10]. Thus we can make the approximation that nuclear matter can be treated as a relativistic uniform isotropic fluid with only irrotational flow, i.e. $\nabla \times \mathbf{v}(\mathbf{x}, t) = 0$. In other words a hydrodynamic treatment of nuclear matter is valid and consistent with our model. So, now we can proceed with the following set of equations

$$-\frac{\partial \Psi}{\partial t} + \frac{1}{2}(\nabla\Psi)^2 + \frac{\mu}{M} = 0 \tag{20}$$

which is Bernoulli's equation from fluid mechanics. Here μ is the chemical potential and is given by

$$\mu = \left(\frac{\partial \varepsilon}{\partial \rho_B}\right)_V = g_V V_0 + (k_F^2 + M^{*2})^{1/2} \tag{21}$$

at equilibrium. We also have the continuity equation for the baryon current

$$\frac{\partial \rho_B}{\partial t} - \nabla \cdot (\rho_B \nabla \Psi) = 0 \tag{22}$$

and the full meson field equations in the MFT are now

$$(\Box^2 + m_V)V_0 = g_V \rho_B \tag{23}$$

$$(\Box^2 + m_s)\phi_0 + \frac{1}{3!}\Omega\phi_0^3 - + \frac{1}{4!}\lambda\phi_0^4 = g_s \rho_s \tag{24}$$

The higher order terms in ϕ_0 in Eq. 24 are not included in the calculations that involve the L2 set of parameters , which makes use of only the linear terms in the Lagrangian. The values of ρ_B and ρ_s can readily be extracted from Eqs. 15 and 19.

We generate the collective modes by introducing small oscillations about equilibrium. To this end, we will expand the dynamical field variables to the first degree about their equilibrium values. The following transformation then occurs

$$k_F = k_{F0} + \delta k_F(\mathbf{x}, t) \tag{25}$$

$$V_0 = V_0 + \delta V_0(\mathbf{x}, t) \tag{26}$$

$$\phi_0 = \phi_0 + \delta\phi_0(\mathbf{x}, t) \tag{27}$$

$$\Psi = \Psi_0 + \delta\Psi(\mathbf{x}, t) \tag{28}$$

Here Ψ is the scalar velocity potential from which we can deduce the vector velocity field through $\mathbf{v}(\mathbf{x}, t) = -\nabla\Psi(\mathbf{x}, t)$ [10]. At equilibrium, we define Ψ to be $\mu_0 t/M$, where μ_0 is the chemical potential , given in Eq. 21. Now we plug Eqs. 25-28 in Eqs. 20 through Eq. 24, and expand everything to first order, dropping the higher order terms. We also impose the following plane wave expansion and normal mode solutions on equations above.

$$\delta\Psi(x) = i\delta\Psi e^{i(\mathbf{k}\cdot\mathbf{x} - \omega t)} \tag{29}$$

$$\delta k_F(x) = \delta k_F e^{i(\mathbf{k}\cdot\mathbf{x} - \omega t)} \tag{30}$$

$$\delta\phi_0(x) = \delta\phi_0 e^{i(\mathbf{k}\cdot\mathbf{x} - \omega t)} \tag{31}$$

$$\delta V_0(x) = \delta V_0 e^{i(\mathbf{k}\cdot\mathbf{x} - \omega t)} \tag{32}$$

Setting $\gamma = 4$ for nuclear matter, we obtain the following set of equations

$$\frac{1}{M}\left(g_V\delta V_0 + \frac{k_F}{E_F}\delta k_F - \frac{M^*}{E_F}g_s\delta\phi_0\right) = \omega\delta\Psi \tag{33}$$

$$k^2\delta\Psi = \omega\frac{3\delta k_F}{k_F} \tag{34}$$

$$(k^2 + m_V^2)\delta V_0 - 2\frac{k_F^2}{\pi^2}g_V\delta k_F = \omega^2\delta V_0 \tag{35}$$

$$(k^2 + m_s^2)\delta\phi_0 - \frac{4g_s}{(2\pi)^3}\left[4\pi k_F^2\frac{M^*}{E_F}\delta k_F - g_s\delta\phi_0\int_0^{k_F}\frac{k^2d^3k}{(\mathbf{k}^2 + M^{*2})^{3/2}}\right]$$
$$+\Omega\phi_0\delta\phi_0 + \frac{1}{2}\lambda\phi_0^2\delta\phi_0 = \omega^2\delta V_0 \tag{36}$$

where $E_F = (k_F^2 + M^{*2})^{1/2}$. Now all the spatial and time dependence of our variables have been fully incorporated into our equations. Here, ω is the frequency of the collective modes, which appears as an eigenvalue in these equations. All we have to do is make these four equations dimensionless and set the determinant of the coefficients of the fluctuations equal to zero. We then solve the resulting polynomial at different momenta k in terms of the frequency. Since $\hbar = c = 1$, all the mass terms, $k_F,\ \omega,\ E_F$ and all the field variables (except $\delta\Psi$, which has units of 1/[energy]) can be given in units of mass. Hence, we can rewrite Eqs. 33 through 36 in terms of dimensionless quantities and variables. Thus, for the field variables, we have the following modifications

$$\frac{g_V\delta V_0}{M} \equiv \delta W_0, \quad \frac{g_s\delta\phi_0}{M} \equiv \delta\Phi_0, \quad \frac{\delta k_F}{M} \equiv \delta\kappa_F, \qquad M\delta\Psi \equiv \delta\Psi \tag{37}$$

The remaining quantities are defined by

$$\frac{M^*}{M} \equiv \chi, \quad \frac{k}{M} \equiv \kappa, \quad \frac{\omega}{M} \equiv \varepsilon, \quad \frac{m_V}{M} \equiv m_V$$
$$\frac{m_s}{M} \equiv m_s, \quad \frac{E_F}{M} \equiv \varepsilon_F, \quad \frac{k_F}{M} \equiv \kappa_F \tag{38}$$

After substituting in the new dimensionless variables above, Eqs. 33 through 36 become

$$\delta W_0 + \frac{\kappa_F}{\varepsilon_F}\delta\kappa_F - \frac{\chi}{\varepsilon_F}\delta\Phi_0 = \varepsilon\delta\Psi \tag{39}$$

$$\kappa^2\delta\Psi = \varepsilon\frac{3\delta\kappa_F}{\kappa_F} \tag{40}$$

$$(\kappa^2+m_V^2)\delta W_0 - 2\frac{g_V^2}{\pi^2}\kappa_F^2\delta\kappa_F = \varepsilon^2\delta W_0 \tag{41}$$

$$(\kappa^2+m_s^2)\delta\Phi_0 - \frac{4g_s^2}{(2\pi)^3}\left[4\pi\kappa_F^2\frac{\chi}{\varepsilon_F}\delta\kappa_F - \delta\Phi_0\int_0^{\kappa_F}\frac{\kappa^2 d^3\kappa}{(\kappa^2+\chi^2)^{3/2}}\right] + \frac{\Omega}{M}\Phi_0\delta\Phi_0 + \frac{\lambda}{2g_s^2}\Phi_0^2\delta\Phi_0 = \varepsilon^2\delta\Phi_0 \tag{42}$$

where the dimensionless Fermi energy is defined to be, $\varepsilon_F = (\kappa_F^2+\chi^2)^{1/2}$

Our remaining task is to solve Eqs. 39-42 for ε. We begin by placing all 4 equations in a 4x4 matrix, and we set the determinant equal to zero to look for non-trivial solutions. The result is a sixth degree polynomial in ε (third in ε^2), which we solve at various momenta, κ. As mentioned earlier, to perform these calculations we adopt 3 different sets of parameters fit to the properties of nuclei: L2, where we set λ and $\Omega = 0$, and NLC and Q1, which are the nonlinear approximations of increasing sophistication in their fit to nuclear properties. The following table[2] displays all the parameters that change as we go from one set to the other. The QHD effective field theory approach to nuclear structure gives an excellent description when using these parameter sets.

Table 1: Dirac-Hartree parameter sets. Note that m_s, and Ω are in MeV

Set	g_s^2	g_V^2	g_ρ^2	m_s	Ω	λ	λ
L2	109.63	190.43	65.23	520	0	0	0.541
NLC	95.11	148.93	74.99	500.8	5000	-200	0.63
Q1	103.61	164.62	77.96	504.6	4570	-197.3	0.63

The g_ρ is the coupling constant for the isovector ρ meson and comes into play when we deal with neutron matter, as will be described later in this paper. The remaining relevant parameters are $m_V = 782$ MeV, M = 939 MeV, and $k_F = 1.42 fm^{-1}$. The reader is encouraged to refer to [1] for a further discussion on these parameters.

[2]Table adapted from [1, 11]

Making use of Table 1, we obtain 3 different sets of solutions, which all behave identically but differ in magnitude, as we will show.

The determinant yields 3 positive roots for each value of κ. They are, in order from the smallest to largest, the zero sound, and the scalar and vector meson field modes. Now that we have obtained numerical approximations for the frequencies of our modes, we can make plots to examine the behavior of ε with respect to κ. Figures 1,2, and 3 are plots of ε vs. κ in L2, NLC, and Q1 respectively. As we have emphasized before, the behavior of the modes is identical in all three cases (except for the slight difference in the amplitudes).

Clearly, the large scalar and vector fields dominate the behavior of the modes and the additional parameters allow for small adjustments of nuclear properties near equilibrium [1].

Our main interest is the zero-sound, which is the lowest-lying mode. To demonstrate the dramatic effect of the of the meson field couplings on the zero sound mode, we let all the coupling constants (g_s and g_V) in Eqs. 39-42 go to 0. The result is the plot in Figure 4, which indicates that in the absence of couplings the zero sound exhibits the linear dispersion behavior, $\omega = |\mathbf{k}|v$. Combining Eqs 33 and 34 for this case enables us to come up with an expression for the frequency (therefore velocity) of zero sound without the couplings, which we can relate to the Fermi velocity by the following relation. Hence, now we can write down an expression for the Fermi velocity of the zero sound

$$\omega_0 = \frac{k_F k}{\sqrt{3ME_F}} = \frac{v_F k}{\sqrt{3}} = v_0 k \tag{43}$$

Inserting the numerical values and solving for v_0 , we get 0.203c for the velocity of the zero sound without the couplings. Once we have coupling of modes, the scalar field and zero sound modes interact and the scalar mode disrupts the linear behavior of the zero sound by pushing it down.

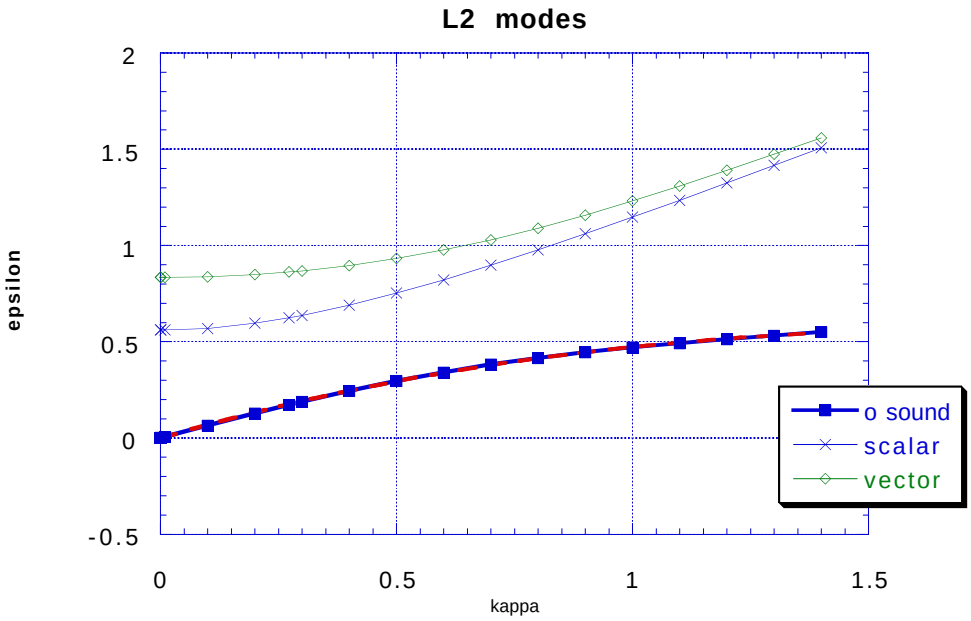

Figure 1: The L2,i.e. linear modes. Here the lowest epsilon mode is the zero sound, which gets pushed down by the scalar meson field, which in turn gets pushed up, V_{ph} slows down to about 0.376c

The phase and group velocities of the modes can readily be obtained from.

$$V_{phase} = \frac{\varepsilon}{\kappa} \tag{44}$$

$$V_{group} = \frac{\partial \varepsilon}{\partial \kappa} \tag{45}$$

We see from Figures 1,2,and 3 that the slope of the zero sound mode gets less steep as values of the wave number, κ get larger, i.e. as κ increases the zero sound slows down. For example, in L2 V_{ph} slows down from a speed of roughly 0.6c to 0.376c. Figure 5 displays the group velocity for all three sets of parameters. Clearly the velocities

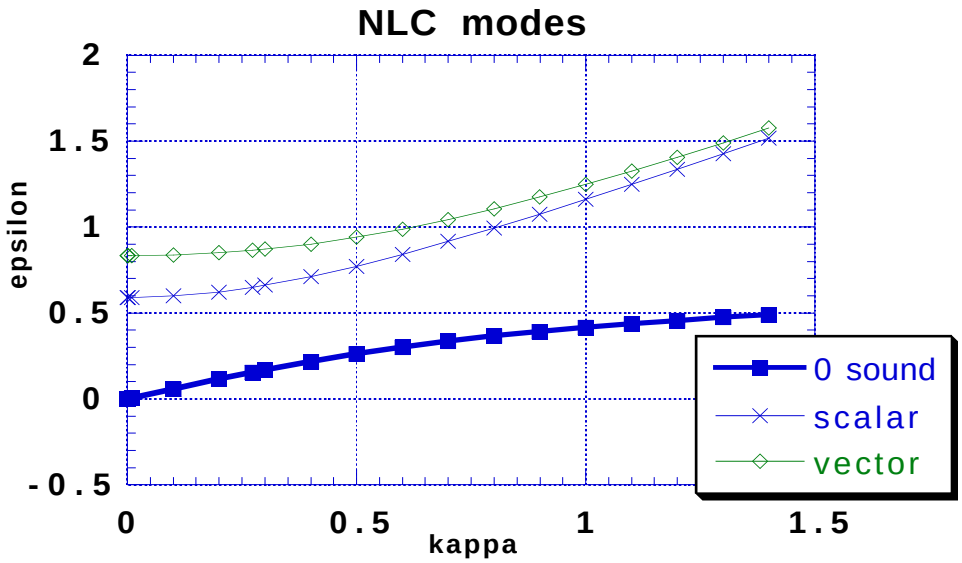

Figure 2: The NLC modes. They exhibit the same behavior as in the case of L2, except the zero sound modes propagates at a smaller velocity as we can tell from the slightly decreased frequencies at various wavelengths, κ. V_{ph} slows down to about 0.336

belonging to all three sets decrease as the wavenumber gets bigger and decay toward the zero sound velocity given in Eq. 43, which represents the case in which we set the coupling constants equal to zero. Looking at Figure 5 closely, we see that the L2 mode predicts the largest values of velocity. The reason for the greater velocity of zero-sound in L2 than in NLC and Q1 originates from the fact that L2 spawns a stiffer model of a nucleus than NLC and Q1. We know that the compressibility of nuclear matter, K is inversely proportional to the speed of the sound waves propagating in it [10]. The greater velocity in L2 implies a smaller K of nucleus in L2 than NLC

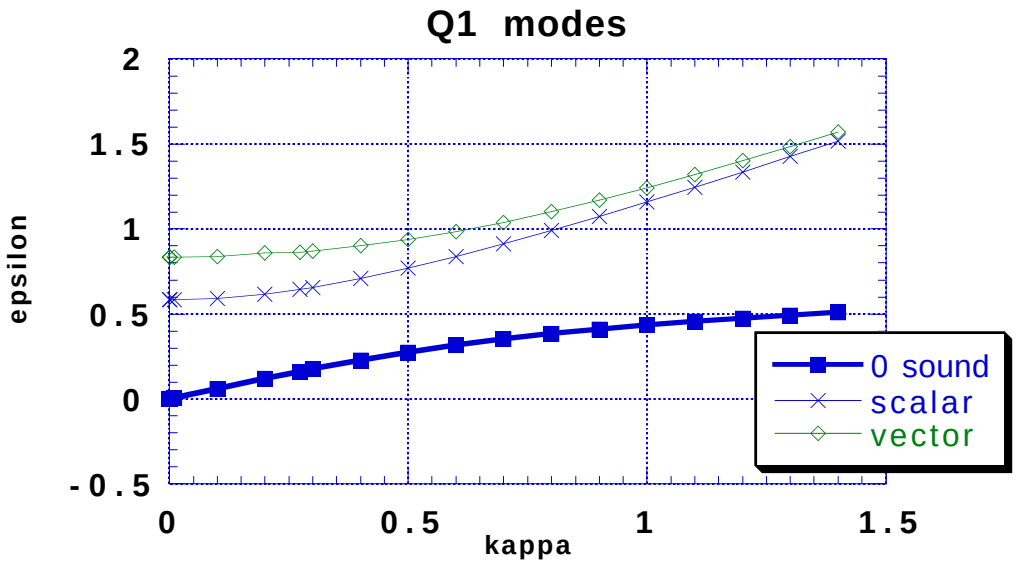

Figure 3: The Q1 modes. The velocity of the zero sound is greater than that in NLC and smaller than that in L2, i.e. the linear case. V_{ph} slows down to about 0.349

and Q1. Therefore nuclear medium based on L2 parameters is less compressible, i.e. stiffer than that of NLC and Q1. The additional small nonlinear terms used in NLC and Q1 rectify this problem by "softening" the nuclear medium.

4.2 NEUTRON MATTER

We follow the same recipe for neutron matter. But our γ factor changes from 4 to 2. More importantly, we have to include a mean field for the isovector ρ meson, b_0, which we need to fit to the nuclear symmetry energy because the repulsive forces in neutron

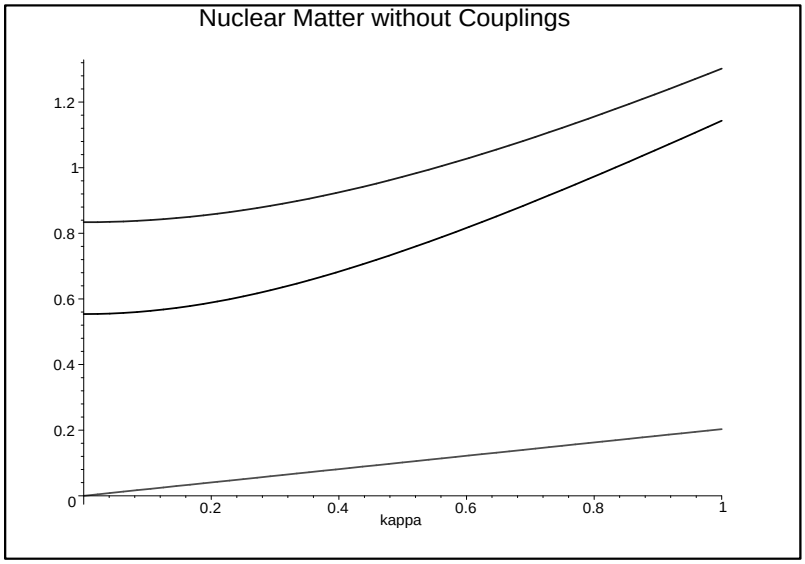

Figure 4: The collective modes without the coupling constants. This implies that we turn off the interaction of the meson fields. As a result we observe entirely a linear behavior for the zero-sound (the initial dispersion relation), which of course vanishes once we turn the meson fields back on.

matter are otherwise underestimated [1]. As a result, our Lagrangian undergoes a few modifications and is given in Refs. [1] and [4] as

$$\mathcal{L}_{MFT} = \frac{1}{2}m_v^2 V_0^2 - \frac{1}{2}m_s^2\phi_0^2 - \frac{1}{3!}\Omega\phi_0^3 - \frac{1}{4!}\lambda\phi_0^4 + \bar{\psi}[i\partial^\mu\gamma_\mu - g_v V_0\gamma_0 - g_\rho\frac{1}{2}\tau_3\gamma_0 b_0 - M^*]\psi \quad (46)$$

Eqs. 39-42 go through the following changes

$$\delta W_0 - \frac{1}{2}\delta B_0 + \frac{\kappa_F}{\varepsilon_F}\delta\kappa_F - \frac{\chi}{\varepsilon_F}\delta\Phi_0 = \varepsilon\delta\Psi \quad (47)$$

$$\kappa^2\delta\Psi = \varepsilon\frac{3\delta\kappa_F}{\kappa_F} \quad (48)$$

$$(\kappa^2 + m_V^2)\delta W_0 - \frac{g_V^2}{\pi^2}\kappa_F^2\delta\kappa_F = \varepsilon^2\delta W_0 \quad (49)$$

$$(\kappa^2 + m_s^2)\delta\Phi_0 - \frac{4g_s^2}{(2\pi)^3}\left[2\pi\kappa_F^2\frac{\chi}{\varepsilon_F}\delta\kappa_F - \frac{\delta\Phi_0}{4}\int_0^{\kappa_F}\frac{\kappa^2 d^3\kappa}{(\kappa^2+\chi^2)^{3/2}}\right] + \frac{\Omega}{M}\Phi_0\delta\Phi_0 + \frac{\lambda}{2g_s^2}\Phi_0^2\delta\Phi_0 = \varepsilon^2\delta\Phi_0 \quad (50)$$

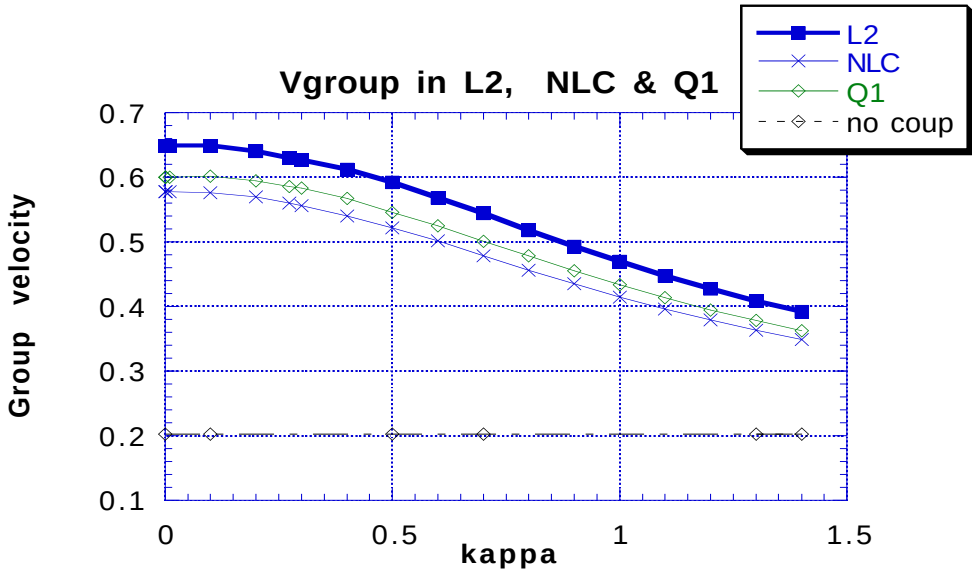

Figure 5: The calculated group velocity of the zero-sound collective mode using the different sets of parameters, L2, NLC, and Q1. Here no coup. means there are no couplings, in other words no coup is the zero sound velocity obtained in Eq. 43.

Here B_0 is the dimensionless ρ meson field and is defined by $g_\rho \delta b_0/M \equiv \delta B_0$. In addition we also have the ρ meson field equation

$$(\omega^2 - k^2 - m_\rho^2) b_0 = -\frac{g_\rho}{2} \bar{\psi} \tau_3 \gamma_0 \psi \tag{51}$$

where τ_3 is the third Pauli isospin matrix, i.e. $\left(\begin{smallmatrix} 1 & 0 \\ 0 & -1 \end{smallmatrix}\right)$. After substituting the dimensionless variables and linearizing, we obtain the additional row meson field equation

$$(\kappa^2 + m_\rho^2)\delta B_0 - \frac{g_\rho^2}{2\pi^2} \kappa_F^2 \delta\kappa_F = \varepsilon^2 \delta B_0 \tag{52}$$

Now we have a 5x5 matrix whose determinant we must evaluate to study the collective modes in neutron matter. The determinant gives rise to an 8th degree polynomial

(fourth order in ε^2), so we actually have 4 different branches[3] of collective modes, the zero sound, scalar, isovector, and vector modes as depicted in Figure 6. Now

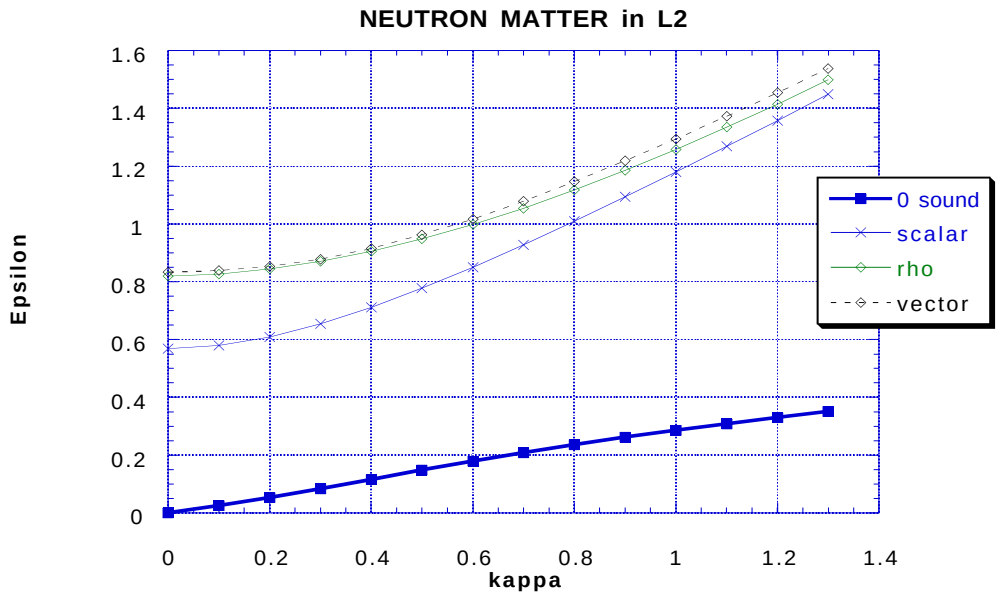

Figure 6: The neutron matter collective modes in L2. Note the additional isovector mode, rho situated right below the vector mode. This new mode spawns a rather interesting change in the propagation of the zero-sound

after calculating the group velocity of the modes for the neutron matter, we find that the zero-sound undergoes a peculiar change. Contrary to our expectations based on results extracted from the nuclear matter study, the zero-sound mode does not immediately slow down in the neutron matter. Instead its velocity first increases, then it starts slowing down and eventually just like the modes propagating in nuclear matter it decays toward the zero sound velocity in absence of the couplings. We have not yet fully explored the possible cause of this mysterious effect, therefore we

[3]We need only keep the positive roots for propagation of the modes as is usual for continuum mechanics

cannot really conclude why neutron matter behaves this way, but clearly it must have something to do with the isovector meson field, ρ

The three meson field equations do not go through any deviation from their original bearing presented in the previous section. They continue to move faster as they penetrate regions of higher κ. Notice that they nearly converge at high wavenumbers, an interesting situation that is not considered in this paper.

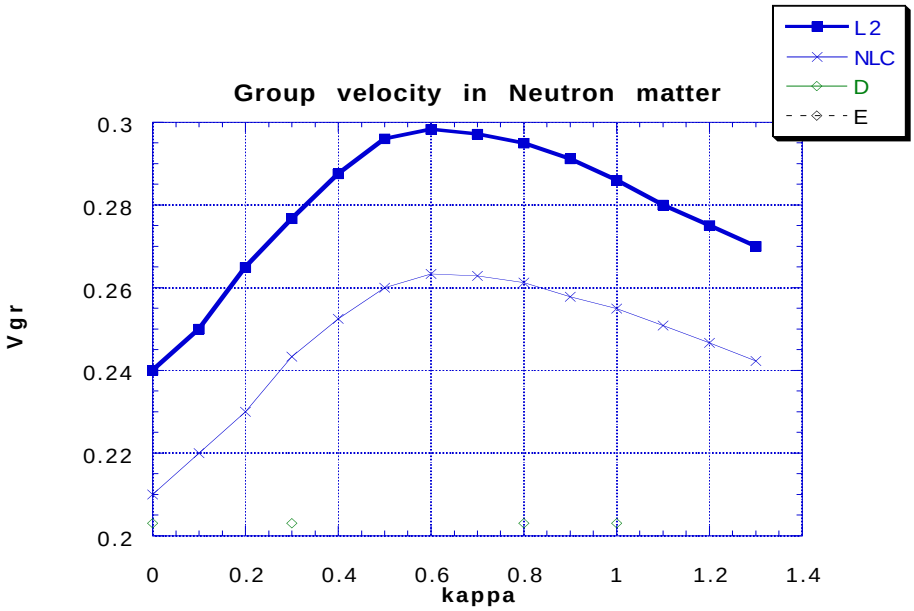

Figure 7: **Group velocity in neutron matter in L2**: The velocities do not immediately decrease as in the case of nuclear matter, they first reach a maximum then decrase. D here represents the velocity of the zero sound without the coupling constants

5 NUMERICAL SOLUTION FOR COLLECTIVE MODES

So far we have analytically studied the propagation of various collective modes in both nuclear and neutron matter and investigated how the collective modes, espe-

cially the zero-sound behave once couplings to the meson fields occur. In this section we focus on actually numerically solving the non-linear second order differential equations presented in the beginning of Section 4.1 . The modes move faster as they move into regions of higher density. This physical fact suggests a non-linearity for finite-amplitude disturbances. As Walecka and Fetter explain in [12] "sound waves should propagate faster in a compressed region than in a rarefied one, with the high-density crests tending to overtake the low-density troughs". We will show later that a distortion of this nature can ultimately produce a shock front. We will first adopt a linear approach in one-dimensional geometry (spatial dimension) to evaluate the vector potential and momentum of the collective modes. Then, we will solve the non-linear differential equations without dropping the higher order terms again in one spatial dimension. The linear case is an approximation to the actual full non-linear case and should reproduce similar results when run properly. Ultimately, we hope to observe the formation of a shock front, which may improve our understanding of how shock waves form and travel in supernovae and neutron stars.

5.1 SOLUTION FOR THE LINEARIZED NON-LINEAR CASE

We begin our analysis with the following assumption; $m_V \to \infty$. The large vector meson mass implies that the vector meson affects only matter at very short distances. We have taken this step to simplify the relevant differential equations. So our assumption is more practical than physical, and it is actually necessary to work with finite m_V. [2] is a detailed work that actually treats nuclear matter under RMFT without the assumptions of infinite vector mass and irrotational flow. Now Eq. 23 reduces to Eq. 11. By substituting Eq. 11 into Eq. 21, Eq. 20 becomes

$$-\frac{\partial \Psi}{\partial t} + \frac{1}{2}(\nabla \Psi)^2 + \frac{1}{M}\left[\frac{g_V^2 \rho_B}{m_V^2} + (k_F^2 + M^{*2})^{1/2}\right] = 0 \tag{53}$$

After inserting Eq. 15 in Eq. 22, Eq. 22 becomes

$$\frac{\partial k_F}{\partial t} = \frac{1}{3k_F^2}\frac{\partial}{\partial x}\left[k_F^3\frac{\partial \Psi}{\partial x}\right] \tag{54}$$

At this stage we switch to dimensionless variables again, that is we reduce everything to dimensions of mass (where $Mx = x$ and $Mt = t$). We also set the parameters Ω and λ to zero for simplicity. We first examine the linearized case. We continue with the same procedure as before; introduce small oscillations around the equilibrium, and mutatis mutandis. In other words after inserting Eqs. 25 through 32 we obtain the following

$$\frac{\partial \delta\Psi}{\partial t} = \frac{C_V^2\gamma\kappa_F^2\delta\kappa_F}{2\pi^2} + \frac{\kappa_F\delta\kappa_F - \chi\delta\Phi_0}{\varepsilon_F} \tag{55}$$

$$\frac{3}{\kappa_F}\frac{\partial \kappa_F}{\partial t} = \nabla^2\delta\Psi \tag{56}$$

$$\delta\Phi_0 = \frac{C_s^2\gamma}{(2\pi)^3}\left[\frac{4\pi\kappa_F^2\delta\kappa_F\chi}{\varepsilon_F} - \delta\Phi_0\int_0^{\kappa_F}\frac{\kappa^2 d^3\kappa}{(\kappa^2+M^{*2})^{3/2}}\right] \tag{57}$$

where the dimensionless coupling constants C_s and C_V are defined as g_sM/m_s and g_VM/m_V respectively. Now we can plug Eq. 57 in Eq. 55 and obtain the following differential equations

$$\frac{\partial \delta\Psi}{\partial t} = \left[\frac{C_V^2\gamma\kappa_F^2}{2\pi^2} + \frac{\kappa_F}{\varepsilon_F} - \frac{C_s^2\gamma\kappa_F^2\chi^2}{2\pi^2\varepsilon_F^2\left[1+\frac{C_s^2\gamma}{(2\pi)^3}\int_0^{\kappa_F}\frac{\kappa^2 d^3\kappa}{(\kappa^2+M^{*2})^{3/2}}\right]}\right]\delta\kappa_F \tag{58}$$

$$\frac{\partial \kappa_F}{\partial t} = \frac{\kappa_F}{3}\nabla^2\delta\Psi \tag{59}$$

Thus, we have reduced Eqs. 20 through 24 to the two coupled linear differential equations given above, which we put in the following simple form

$$\frac{\partial \delta\Psi}{\partial t} = a\delta\kappa_F \tag{60}$$

$$\frac{\partial \kappa_F}{\partial t} = b\nabla^2\delta\Psi \tag{61}$$

Naturally we look for solutions of the form of sines and cosines. It turns out if we let

$$\delta\Psi = \delta\Psi_0\sin\kappa(x - v_{ph}t) \tag{62}$$

$$\delta\kappa_F = \delta\kappa_0\cos\kappa(x - v_{ph}t) \tag{63}$$

we can solve Eqs. 60 and 61. The substitution above yields $v_{ph} = (ab)^{1/2}$. Now, we are able to procure the numerical value for the phase velocity of this wave travelling right in 1-D. We make use of Table 1 and evaluate everything at $\chi = 0.537$ and $\kappa_F = 0.274$, which in turn gives $a = 0.7395, b = 0.0913$ and $v_{ph} = 0.2598$. The task at hand is to *numerically* solve Eqs. 60 and 61 by imposing the periodic boundary condition, $x = x + L$ with the following initial values

$$\delta\Psi = \delta\Psi_0 \sin(\kappa x) \tag{64}$$

$$\delta\kappa_F = \delta\kappa_0 \cos(\kappa x) \tag{65}$$

in which the amplitudes $\delta\Psi_0$ and $\delta\kappa_0$ can be related through

$$\frac{\delta\Psi_0}{\delta\kappa_0} = -\left(\frac{a}{b}\right)^{1/2} \frac{1}{\kappa} \tag{66}$$

at t=0. Using the conditions stated above, we choose the appropriate time and length intervals, which we slice into very small pieces [Appendix C]. Then we let Maple and Mathcad carry out the calculations and plot the desired wave at the desired time for us. The result is the following two plots.

The conclusion is that once we linearize the equations, we obtain a nice permanent linear behavior, which we have demonstrated both by solving the system analytically Eqs. 60 and 61, which yield the Eqs. 64 and 65 as the solutions , by solving it numerically as shown in Figs. 8 and 9.

5.2 SOLUTION FOR THE FULL NON-LINEAR CASE

This section is allotted to solving the full non-linear equations and investigating their behavior. Again, we begin our analysis with Eqs. 20 through 24, and proceed with the same assumptions as in the previous section. Hence, as before we reduce Eqs .20 through 24 to Eqs. 53 and 54. Our goal is to solve the full set of self-consistent non-linear equations *numerically* and we are no longer restricted to only small oscillations about the equilibrium. After reducing everything to the dimensions of mass, i.e.

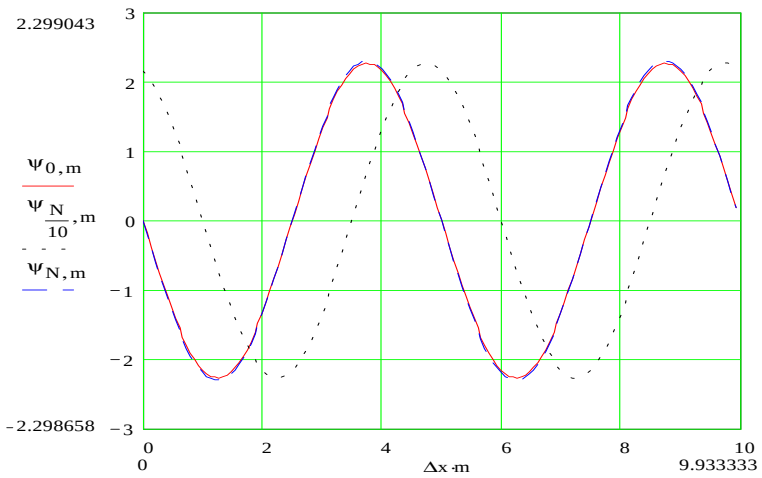

Figure 8: **The velocity potential with respect to position**: Here we have made the wave go around once. Notice that we numerically reproduce the analytic solution stated in Eq. 64

following the prescription to which we have been adhering from the beginning. Eq. 53 remains unaltered after these changes. As for Eq. 54, we perform the differentiation on the right side as before but, this time we do not discard the higher order terms. So Eq. 54 now is

$$\frac{\partial \kappa_F}{\partial t} = \frac{\kappa_F}{3}\frac{\partial^2 \psi}{\partial x^2} + \frac{\partial \kappa_F}{\partial x}\frac{\partial \Psi}{\partial x} \tag{67}$$

We now define $\Psi = -\mu(\kappa_F^0)/M - \delta\Psi(x,t)$ as before, which merely reflects our choice of gauge. We also expand the Fermi wavenumber as $\kappa_F = \kappa_F^0 + \delta\kappa_F(\mathbf{x},t)$, where κ_F^0 represents the equilibrium value. So the full set of non-linear equations becomes

$$\frac{\partial \delta\Psi}{\partial t} = \frac{1}{2}(\nabla\delta\Psi)^2 + \mu(\kappa_F) - \mu(\kappa_F^0) \tag{68}$$

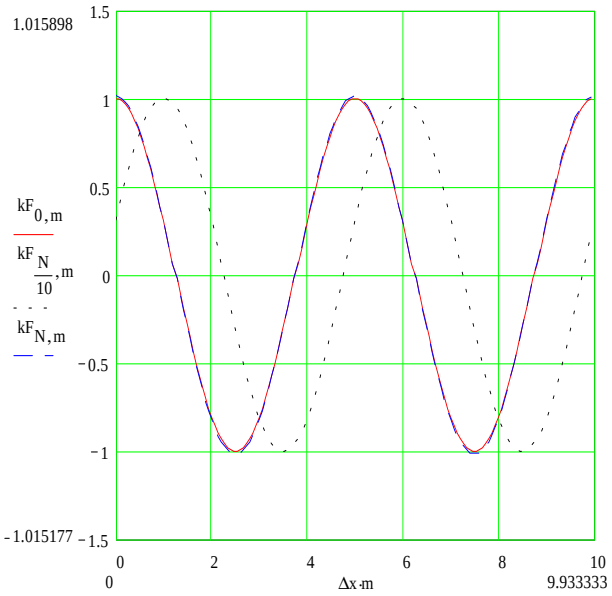

1 Cihan_Waveeqn.mcd
5/9/02
10:18 PM

Figure 9: **The Fermi wave-number** (proportional to the Fermi momentum and baryon density) **vs.position**: Again we nicely approximated the actual solution for $\delta\kappa$ given in Eq. 65

$$\frac{\partial \delta\kappa_F}{\partial t} = \frac{\kappa_F}{3}\frac{\partial^2 \delta\psi}{\partial x^2} + \frac{\partial \delta\kappa_F}{\partial x}\frac{\partial \delta\Psi}{\partial x} \tag{69}$$

Here μ is the chemical potential, which for nuclear matter is

$$\mu(\kappa_F) = \frac{C_V^2 \gamma \kappa_F^3}{6\pi^2} + (\kappa_F^2 + \chi(\kappa_F)^2)^{1/2} \tag{70}$$

where $\chi(\kappa_F)$ is the solution to the dimensionless self-consistent relation in Eqs. 18, 19, given by

$$1 - \chi = \frac{C_s^2 \gamma}{2\pi^3}\rho_s \tag{71}$$

$$\rho_s = \frac{\gamma}{(2\pi)^3}\int_0^{\kappa_F} d^3\kappa \frac{\chi}{(\kappa^2 + \chi^2)^{1/2}} \tag{72}$$

in the case where $\lambda = \Omega = 0$. We input the same initial conditions as before, and use the amplitude of the waves, $\delta\kappa_F$ as an adjustable parameter in evaluating the propagation of the mode. Our Mathcad code manages the rest[Appendix C].

We have previously asserted that the linear approach to solving these non-linear equations is an accurate approximation to solving the actual non-linear case. Thus, it is absolutely imperative that we be able to recover the results depicted in Figures 8 and 9 initially. The two curves displayedin Figs 10 and 11 are results to the full non-linear problem evaluated for one full trip, *i.e.* the wave has only gone around once. Here, we assume a small amplitude $\delta\kappa_0 = 0.0001$. Note that $\delta\psi_0$ is also expressed in terms of $\delta\kappa_0$ by the use of Eq. 66.

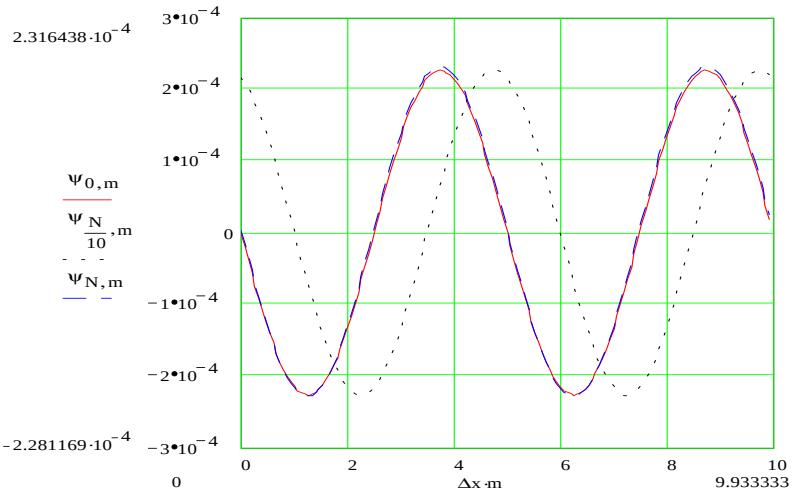

Figure 10: **The velocity potential in the full non-linear case**: with a small given amplitude we observe that the produced wave in this case is identical to the curve in Fig. 10.

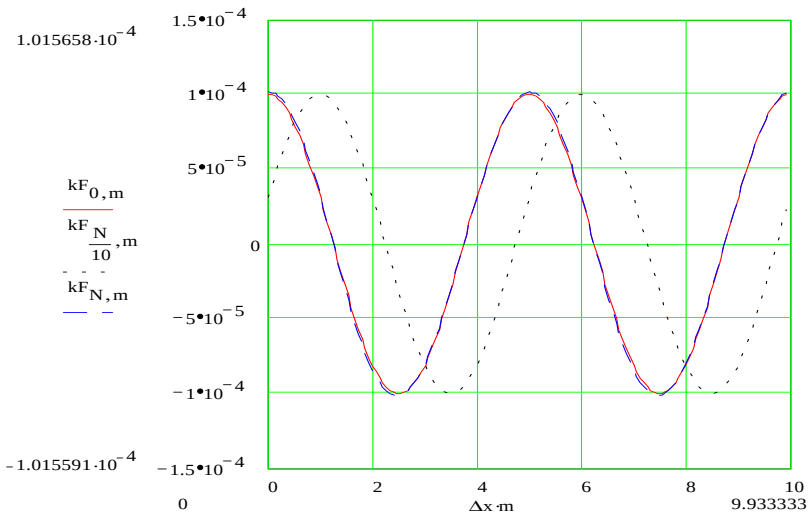

Figure 11: **The fermi wave-number** (proportional to the Fermi momentum and baryon density) **in the full non-linear case**: For small oscillations, we observe an identical behavior to the fermi wave-number evaluated in section 5.1.

It turns out nonlinearity in hydrodynamic systems changes the form of a finite-amplitude sound wave [12] and amplifies it drastically. Eventually the wavefront becomes discontinuous, and the previous description fails. Looking closely at the plots in Figs 12 and 13 we clearly see that the velocity potential is now shifted up, which indicates a net flow of velocity in the proper direction. Notice the sharp peaks of the Fermi momentum, which originate from the fact that at large amplitudes the top of the wave travels faster than the bottom because the shifted velocity potential favors one direction over the other. Eventually the momentum ceases to be a single-valued function. This transition signals the formation of a shock wave as we see in

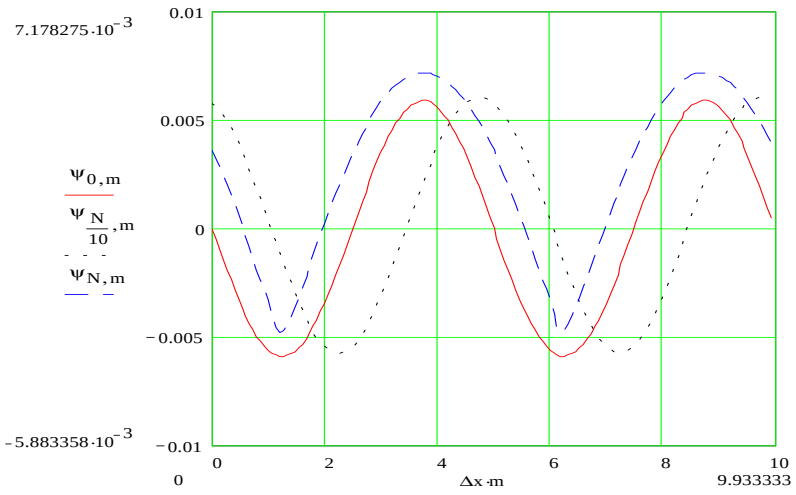

Figure 12: **The velocity potential in the full non-linear case**: Here the amplitude $\delta\kappa_0 = 0.0026$, it is 26 times larger than before. This drastic increase in the amplitude triggers a clear displacement of the velocity potential which indicates to us that there is a net flow of velocity

Fig. 13. The Figs 12 and 13 are calculated starting from a large initial amplitude $\delta\kappa_0 = 0.026$. The same effect is observed if one starts from a smaller amplitude and lets the wave propagate for a long time.

Note that our analyses can be applied to neutron matter as well. All one has to do is to change the γ factor to 2 and incorporate the isovector meson field in Eqs. 53 and 54.

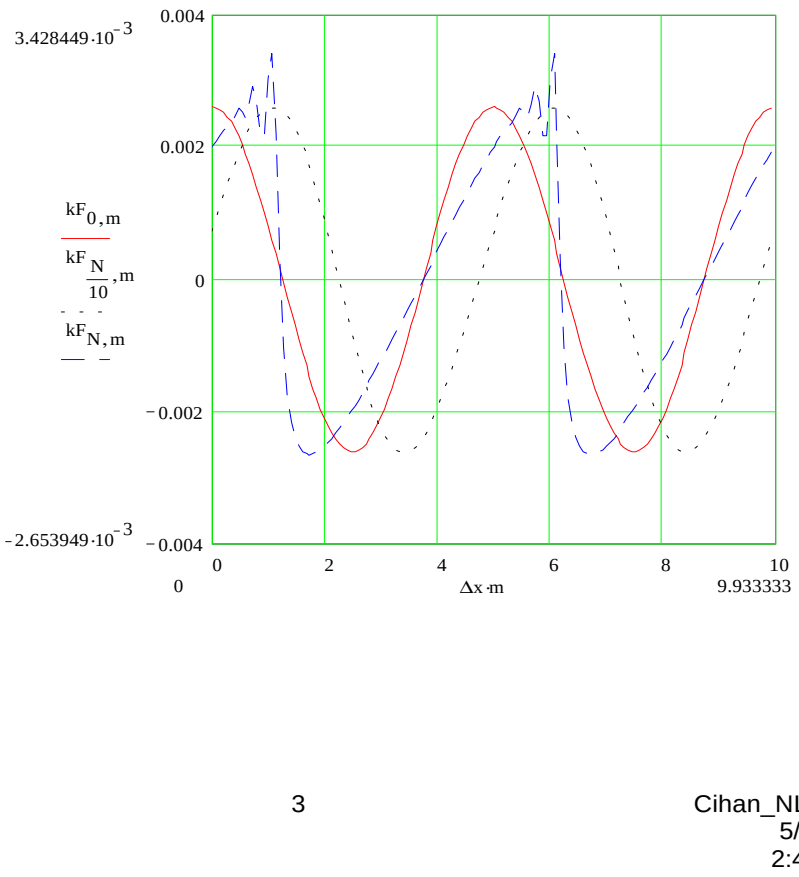

Figure 13: **The Fermi wave-number (proportional to the Fermi momentum, and density) in the full non-linear case**: We see that the wave ,after going around once, begins to transform into a shock wave. If we let it run a for long time the top will eventually crash just like oceanic waves travelling to the beach and crashing when they arrive there

6 CONCLUSIONS

In an attempt to study the elementary excitations of nuclear matter, we have investigated the relativistic propagation of zero-sound waves and other collective modes in the approximation that nuclear matter could be treated as an isotropic and irrotational fluid moving with flow velocity, **v**. We have calculated the Fermi velocity and the zero-sound velocity of the nuclear matter and shown that as we move to regions of greater wave number the group and phase velocities of zero-sound in L2, NLC, and

Q1 decay toward what we called the zero sound velocity in the absence of the meson field couplings. We have seen that the linear calculation leads to a model of nuclear matter that is unrealistically incompressible, which we remedy by using additional non-linear terms in the MFT lagrangian for NLC and Q1 calculations.

We have also applied the same method to neutron matter with a few modifications and obtained a 4-branch collective-mode diagram, displaying the zero sound, scalar, isovector and vector modes, which seem to behave in the same way as the collective modes in nuclear matter. We have discovered that the velocity of the zero-sound in neutron matter behaves differently from that in nuclear matter, mainly due to the coupling with an additional isovector meson field, ρ utilized to improve the symmetry energy.

After studying the collective modes in nuclear and neutron media, we set out to solve the actual non-linear differential equations that describe the propagation of the modes in nuclear matter. Using numerical methods we have solved these equations, first by linearization then by retaining the higher order terms, i.e. solving the full set of non-linear equations . From the results acquired above we extrapolated that the linear version is just an initial model of the non-linear case as we postulated. We have solved numerically the full coupled self-consistent zero-sound equations and demonstrated the cresting of the wave. We have thus arrived at the fascinating conclusion that for an isentropic small-amplitude wave, no matter how small the initial amplitude the non-linearities dominate the behavior of the propagation and eventually culminate in the formation of a shock wave.

APPENDIX

A The Energy of the Nuclear Matter

The Hamiltonian of a system can be extracted through a Legendre transformation: $\Pi_q(\partial q/\partial t) - (L)$ where q is an arbitrary field variable. For the system we are studying we use the following Legendre transformation

$$H = \pi_\psi \dot{\psi} + \pi_{\psi^\dagger} \dot{\psi^\dagger} - \mathcal{L} \tag{73}$$

with conjugate fields defined as

$$\pi_\psi = \frac{\partial \mathcal{L}}{\partial(\partial\psi/\partial t)} = i\psi^\dagger \tag{74}$$

$$\pi_{\psi^\dagger} = \frac{\partial \mathcal{L}}{\partial(\partial\psi^\dagger/\partial t)} = 0 \tag{75}$$

Using Shrödinger picture where operators are time independent and state vectors are time dependent, we expand the baryon field operator in a complete set of solutions to quantize the baryon field [9]

$$\hat{\psi}(\mathbf{x}) = \frac{1}{\sqrt{V}} \sum_{\mathbf{k}\lambda} [U(\mathbf{k}\lambda) A_{\mathbf{k}\lambda} e^{i\mathbf{k}\cdot\mathbf{x}} + \mathcal{V}(-\mathbf{k}\lambda) B^\dagger_{\mathbf{k}\lambda} e^{-i\mathbf{k}\cdot\mathbf{x}}] \tag{76}$$

where V is the volume, U and $\mathcal{V}$ are the Dirac spinors corresponding to E_+ and E_-, and $A^\dagger$, $B^\dagger$, A and B are creation and destruction operators for baryons and anti-baryons respectively. These operators obey the equal-time anti-commutation relations. Using the operators defined above, we can now write down the quantized Hamiltonian [9]

$$\hat{H} - \langle 0|\hat{H}|0\rangle \equiv \hat{H}_{MFT} + \delta H \tag{77}$$

$$\begin{aligned} \hat{H}_{MFT} = &\sum_{\mathbf{k}\lambda} (\mathbf{k}^2 + M^{*2})^{1/2} (A^\dagger_{\mathbf{k}\lambda} A_{\mathbf{k}\lambda} + B^\dagger_{\mathbf{k}\lambda} B_{\mathbf{k}\lambda}) + g_v V_0 \hat{\rho_B} \\ &+ (\frac{1}{2} m_s^2 \phi_0^2 + \frac{1}{3!}\Omega\phi_0^3 + \frac{1}{4!}\lambda\phi_0^4 - \frac{1}{2} m_v^2 V_0^2) V \end{aligned} \tag{78}$$

where

$$\delta H = -\sum_{\mathbf{k}\lambda}[(\mathbf{k}^2 + M^{*2})^{1/2} - (\mathbf{k}^2 + M^2)^{1/2}] \quad (79)$$

$$\hat{\rho_B} = (A^\dagger_{\mathbf{k}\lambda} A_{\mathbf{k}\lambda} - B^\dagger_{\mathbf{k}\lambda} B_{\mathbf{k}\lambda}) \quad (80)$$

B Pressure

The first law of thermodynamics is dE = -pdV with B fixed. Consider [9]

$$\frac{\partial \varepsilon}{\partial \rho_B} = \frac{\partial (E/V)}{\partial V}\frac{\partial V}{\partial \rho_B} = \left(\frac{-E}{V^2} + \frac{1}{V}\frac{\partial E}{\partial V}\right)\left(\frac{-V^2}{B}\right) = \frac{\varepsilon}{\rho_B} + \frac{p}{\rho_B} \quad (81)$$

where

$$\frac{\partial V}{\partial \rho_B} = \frac{1}{B}\frac{\partial V}{\partial (1/V)} = \frac{-V^2}{B} \quad (82)$$

So we can then solve for pressure by rewriting Eq. 81, which becomes

$$p = \rho_B(\partial \varepsilon / \partial \rho_B) - \varepsilon \quad (83)$$

Hence, we can now deduce the expression for pressure given in Eq. 17.

C The Numerical Solution to the Linearized Case

In this section we illustrate how to numerically solve the linearized differential equations given in Eqs. 60 and 61. We define a periodic boundary condition, x = x + L, and divide this length L into many tiny intervals, Δx, 150 in this case. We define total time by τ and also slice the total time into Δt pieces, 5000 in this case. So we have the following relations

$$\Delta x = \frac{L}{M} \quad (84)$$

$$\Delta t = \frac{L\gamma}{v_{ph} N} \quad (85)$$

The boundary condition implies that x + NΔ x = x .

These modifications described above transform the differential equation into an n× m matrix, where n runs from 0 to N - 1, and m from 0 to M - 1. The initial conditions for the two differential equations can be written as (here we have suppressed the δ's for notational brevity)

$$\kappa_{[0,m]} = \cos(2\pi\frac{\Delta x.m}{\lambda}) \quad (86)$$

$$\psi_{[0,m]} = \frac{-\lambda}{2\pi}\sin\left(2\pi\frac{\Delta x.m}{\lambda}\right) \quad (87)$$

with

$$\kappa_{[n,0]} = \kappa_{[n,M]} \quad (88)$$

$$\psi_{[n,0]} = \psi_{[n,M]} \quad (89)$$

Now we can transform the differential equations into matrix elements by

$$\kappa_{[n+1,m]} = \kappa_{[n,m]} + \frac{\Delta t}{\Delta x^2}(\psi_{[n,m+1]}\ if\ m \leq M-2 + \psi_{[n,m-1]}\ if\ m \geq 1\ -2\psi_{[n,m]}) \quad (90)$$

$$\kappa_{[n+1,m]} = \kappa_{[n,m]} + \frac{\Delta t}{\Delta x^2}(\psi_{[n,0]}\ otherwise\ +\psi_{[n,M-1]}\ otherwise\ -2\psi_{[n,m]}) \quad (91)$$

$$\psi_{[n+1,m]} = \psi_{[n,m]} + \Delta\kappa_{[n,m]} \quad (92)$$

Hence, we can choose any n, and construct an n× M matrix, and see how the wave travels to get to the selected time index. Note that the non-linear case uses the identical initial and boundary conditions as the linear case. But in the non-linear (solving the full differential equations) we have to include the wave amplitude $\delta\kappa_F$ as an input parameter in order to amplify the wave . Because we concluded that the wave keeps building up for the non-linear case, and after it has reached a certain amplitude a shock wave forms. All we have to do is to apply the recipe described in this section to Eqs. 68 and 69 and calculate the matrix elements using of course the additional non-linear terms.

References

[1] J.D. Walecka and B.D. Serot,"Recent Progress in Quantum Hadrodynamics," International Journal of Modern Physics **E 6** 4, 515-631, (1997)

[2] C. da Providência, L. Brito, J. da Providência, M. Nielsen, X. Viñas, "A Relativistic Thomas-Fermi Description of Collective Modes in Droplets of Nuclear Matter," Phys. Rev. **C**, **1**, (05/24/1996)

[3] L. Brito and J. da Providência, Phys. Rev. **C32**, 2049 (1985)

[4] B.D. Serot and J.D. Walecka *Advances in Nuclear Physcis* **16** 1 (1986)

[5] J.D. Walecka, "Equation of State for Neutron Matter at Finite T in a Relativistic Mean-Field Theory," Phys. Lett. **59B**, 2, 24-28 (10/27/1975)

[6] J. D. Walecka and A. L. Fetter. *Quantum Theory of Many Particle Systems.*McGraw-Hill Inc., (1971)

[7] J.D. Walecka and B.D. Serot,"Effective Theory in Nuclear Many-Body Physics," 150 Years of Quantum Many-Body Theory, World Scientific Publishing Co. Pte. Ltd., (2001)

[8] S.A. Chin, J.D. Walecka, "An Equation of State for Nuclear and High-Density Matter Based on a Relativistic Mean-Field Theory," Phys. Lett. **52B**, 1, 24-28, (09/16/1974)

[9] J.D. Walecka *Theoretical Nuclear and Subnuclear Physics*. Oxford University Press, NY, (1995)

[10] W.E.Kleppinger, "Relativistic Hydrodynamics in a Mean-Field Theory of Nuclear Matter," Acta Polonica **B13**, 607-15, (1982)

[11] R.J.Furnstahl, B.D. Serot, and H.-B. Tang, *Nucl. Phys.* **A598**, 539 (1996)

[12] J. D. Walecka and A. L. Fetter. *Theoretical Mechanics of Particles and Continua*. McGraw-Hill Inc., (1980)